Chapter 10
Methods for the Simulation of Coupled Electronic and Nuclear Motion in Molecules Beyond the Born-Oppenheimer Approximation

Erik Lötstedt, Tsuyoshi Kato and Kaoru Yamanouchi

Abstract We review theoretical methods which can be used for the simulation of time-dependent electronic and nuclear dynamics of gas-phase molecules beyond the Born-Oppenheimer approximation. We concentrate on methods which allow for a description of extensive electronic excitation and ionization. Particular emphasis is placed on the extended multiconfiguration time-dependent Hartree-Fock (Ex-MCTDHF) method. We provide a derivation of the equations of motion of the Ex-MCTDHF method, and discuss its advantages and disadvantages over the methods based on the Born-Huang expansion.

10.1 Introduction

When molecules are irradiated with intense laser light, one or more electrons in the molecule absorb energy from the laser pulse. The motion of electrons is excited and the electrons can be ejected from molecules, and the molecules as well as the resulting molecular ions can be electronically and/or vibrationally excited. The acquired energy is subsequently transferred to the nuclei, which triggers a variety of nuclear motion within the molecule: vibrational motion, structural deformation, and dissociation. An interesting example is a process called hydrogen migration, in which a hydrogen atom or a proton in an excited molecule moves in the wide spatial range within the molecule on a fast time scale. In [1, 2], the hydrogen migration process in methanol was studied. In [1], it was revealed that, after the ionization $CH_3OH \rightarrow CH_3OH^+$ of a methanol molecule by an 800 nm, 60 fs laser pulse, a hydrogen atom moves within a molecule, so that CH_2^+ and OH_2^+ fragments are formed af-

E. Lötstedt (✉) · T. Kato · K. Yamanouchi
Department of Chemistry, School of Science, The University of Tokyo, 7-3-1 Hongo, Bunkyo-ku, Tokyo 113-0033, Japan
e-mail: lotstedt@chem.s.u-tokyo.ac.jp

T. Kato
e-mail: tkato@chem.s.u-tokyo.ac.jp

K. Yamanouchi
e-mail: kaoru@chem.s.u-tokyo.ac.jp

K. Yamanouchi et al. (eds.), *Progress in Photon Science*, Springer Series in Chemical Physics 119, https://doi.org/10.1007/978-3-030-05974-3_10

ter a double ionization. The hydrogen migration was found to proceed within the laser pulse, that is, on a time scale shorter than 60 fs. By employing a pump-and-probe scheme, the time scale of the hydrogen migration was found to be shorter than 25 fs [2].

Another example is the experiments on the asymmetric dissociation of H_2 into H + H^+ or H^+ + H [3, 4], in which H_2 is first ionized to H_2^+ by a short laser pulse, and then, in the course of the dissociation of H_2^+, the remaining electron is driven by the later part of the laser field so that it ends up with being caught by either one of the two protons. It was shown that the final position of the electron (on the left proton or on the right proton) could be controlled by varying the carrier-envelope phase of the driving laser field. We stress that ionization, electronic excitation and dissociation in this case proceed within the same laser pulse.

The complex interplay between electronic excitation, ionization, and nuclear motion has also been shown in experiments on other molecular species, such as I_2 [5], N_2 [6], H_3^+ [7], and C_4H_6 [8, 9].

In order to interpret the experimental results showing that laser-driven molecules undergo complex dynamical processes such as electronic excitation, ionization, nuclear vibration and dissociation, we need to develop a theoretical framework in which both electronic and nuclear motion are included in a general way without imposing any constraints on the electronic motion and the nuclear motion, so that arbitrary electronic excitation (including ionization) and nuclear motion (including dissociation) can be simulated. Presently, an efficient quantum mechanical method fulfilling fully these requirements has not been known. However, a few attempts have been made along this direction in these years. In this article, we first review in Sect. 10.2 the standard theoretical method for dealing with laser-molecule interaction based on the Born-Oppenheimer (BO) approximation. After discussing the advantages and the disadvantages of the BO approximation, we will review several attempts at going beyond the BO approximation. In Sect. 10.3, we give a detailed account of the extended multiconfiguration time-dependent Hartree-Fock (Ex-MCTDHF) method, including a derivation of the equations of motion. In the remaining sections, we provide brief overviews of three related methods, i. e., the multiconfiguration time-dependent Hartree (MCTDH) method (Sect. 10.4.1), the multi-configuration electron-nuclear dynamics (MCEND) method (Sect. 10.4.2), and the MCTDHF method for diatomic molecules (Sect. 10.4.3).

10.2 Born-Oppenheimer Approximation

The BO approximation is the standard method for simulating laser-molecule interaction. In order to derive the working equations for the BO approximation [10], we start with the Hamiltonian of a general molecule consisting of N_e electrons with mass m_e and N_N nuclei with masses M_k and charge numbers Z_k ($k = 1, \ldots, N_N$),

$$H = T_N + V_{NN} + U_N(t) + H_e + U_e(t), \tag{10.1}$$

where

$$T_{\mathrm{N}} = \sum_{k=1}^{N_{\mathrm{N}}} \frac{-\hbar^2}{2M_k} \nabla^2_{\mathbf{R}_k} \tag{10.2}$$

is the nuclear kinetic energy operator with $\mathbf{R}_k$ denoting the spatial coordinate of nucleus k,

$$V_{\mathrm{NN}} = \sum_{k=1}^{N_{\mathrm{N}}} \sum_{l<k} \frac{Z_k Z_l e^2}{4\pi\varepsilon_0 |\mathbf{R}_k - \mathbf{R}_l|} \tag{10.3}$$

is the nuclear-nuclear repulsive Coulomb potential,

$$U_{\mathrm{N}}(t) = -\sum_{k=1}^{N_{\mathrm{N}}} Z_k e \mathbf{E}(t) \cdot \mathbf{R}_k \tag{10.4}$$

is the nuclear-laser interaction expressed in the dipole approximation with the laser field $\mathbf{E}(t)$,

$$H_{\mathrm{e}} = \sum_{k=1}^{N_{\mathrm{e}}} \left(\frac{-\hbar^2}{2m_{\mathrm{e}}} \nabla^2_{\mathbf{r}_k} - \sum_{l=1}^{N_{\mathrm{N}}} \frac{Z_l e^2}{4\pi\varepsilon_0 |\mathbf{r}_k - \mathbf{R}_l|} + \sum_{l<k} \frac{e^2}{4\pi\varepsilon_0 |\mathbf{r}_k - \mathbf{r}_l|} \right) \tag{10.5}$$

is the electronic Hamiltonian with $\mathbf{r}_k$ denoting the spatial coordinate of electron k, and

$$U_{\mathrm{e}}(t) = \sum_{k=1}^{N_{\mathrm{e}}} e \mathbf{E}(t) \cdot \mathbf{r}_k \tag{10.6}$$

is the electron-laser interaction. In the following discussion, we introduce for convenience a collective coordinate $\overline{\mathbf{R}} = (\mathbf{R}_1, \mathbf{R}_2, \ldots, \mathbf{R}_{N_{\mathrm{N}}})$ to denote the spatial coordinates of all the nuclei, and similarly $\overline{\mathbf{r}} = (\mathbf{r}_1, \mathbf{r}_2, \ldots, \mathbf{r}_{N_{\mathrm{e}}})$ for the electrons. We also define the spin coordinate of electron k as s_k, the combined spatial-spin coordinate as $x_k = (\mathbf{r}_k, s_k)$, and the collective spin-spatial coordinate as $\overline{x} = (x_1, x_2, \ldots, x_{N_{\mathrm{e}}})$

In the BO approximation, we first construct a set of L_{BO} electronic states $\Phi_j(\overline{x}; \overline{\mathbf{R}})$, $j = 1, 2, \ldots, L_{\mathrm{BO}}$, which parametrically depends on the nuclear coordinate $\overline{\mathbf{R}}$. The electronic states are calculated by solving the eigenvalue equation

$$\mathscr{E}_j(\overline{\mathbf{R}}) \Phi_j(\overline{x}; \overline{\mathbf{R}}) = H_{\mathrm{e}}(\overline{\mathbf{R}}) \Phi_j(\overline{x}; \overline{\mathbf{R}}), \tag{10.7}$$

where $\overline{\mathbf{R}}$ is treated as a set of parameters $(\mathbf{R}_1, \ldots, \mathbf{R}_{N_{\mathrm{N}}})$ taking fixed values. Because H_{e} is Hermitian, the electronic states are orthogonal. We have $\int \Phi^*_j(\overline{x}; \overline{\mathbf{R}}) \Phi_k(\overline{x}; \overline{\mathbf{R}}) \mathrm{d}\overline{x} = \delta_{jk}$ after appropriate normalization. Equation (10.7) has to be solved at each value of the nuclear coordinate $\overline{\mathbf{R}}$, which may become a difficult task for large molecules. This point is discussed more in detail later at the end of this section.

We make the ansatz here

$$\Psi(\overline{\mathbf{R}}, \overline{x}, t) = \sum_{j=1}^{L_{\mathrm{BO}}} \chi_j(\overline{\mathbf{R}}, t) \Phi_j(\overline{x}; \overline{\mathbf{R}}) \tag{10.8}$$

for the total wave function. The expansion (10.8) is commonly referred to as the Born-Huang (BH) expansion [11]. The time-dependence of the wave function is contained in the nuclear wave functions $\chi_j(\overline{\mathbf{R}}, t)$. Inserting the ansatz (10.8) into the time-dependent Schrödinger equation (TDSE)

$$\mathrm{i}\hbar \frac{\partial \Psi(\overline{\mathbf{R}}, \overline{x}, t)}{\partial t} = H \Psi(\overline{\mathbf{R}}, \overline{x}, t) \tag{10.9}$$

and integrating out the electronic degrees of freedom leads to a set of coupled equations for the nuclear wave functions,

$$\begin{aligned} \mathrm{i}\hbar \frac{\partial \chi_j(\overline{\mathbf{R}}, t)}{\partial t} &= \left(T_{\mathrm{N}} + U_{\mathrm{N}}(t) + V_j^{\mathrm{BO}}(\overline{\mathbf{R}})\right) \chi_j(\overline{\mathbf{R}}, t) \\ &\quad + \sum_{k=1}^{L_{\mathrm{BO}}} \left(-\mathbf{E}(t) \cdot \boldsymbol{\mu}_{jk}(\overline{\mathbf{R}}) + A_{jk} + B_{jk}\right) \chi_k(\overline{\mathbf{R}}, t), \end{aligned} \tag{10.10}$$

where

$$V_j^{\mathrm{BO}}(\overline{\mathbf{R}}) = \mathscr{E}_j(\overline{\mathbf{R}}) + V_{\mathrm{NN}}(\overline{\mathbf{R}}) \tag{10.11}$$

is a BO potential energy surface defined using the electronic eigenenergy in (10.7),

$$\boldsymbol{\mu}_{jk}(\overline{\mathbf{R}}) = -e \int \mathrm{d}\overline{x} \Phi_j^*(\overline{x}; \overline{\mathbf{R}}) \left(\sum_{l=1}^{N_{\mathrm{e}}} \mathbf{r}_l \right) \Phi_k(\overline{x}; \overline{\mathbf{R}}) \tag{10.12}$$

is the transition dipole matrix element, and

$$A_{jk} = -\hbar^2 \int \mathrm{d}\overline{x} \Phi_j^*(\overline{x}; \overline{\mathbf{R}}) \left(\sum_{l=1}^{N_{\mathrm{N}}} \frac{\nabla_{\mathbf{R}_l}}{M_l} \right) \Phi_k(\overline{x}; \overline{\mathbf{R}}) \cdot \nabla_{\mathbf{R}_l} \tag{10.13}$$

and

$$B_{jk} = -\frac{\hbar^2}{2} \int \mathrm{d}\overline{x} \Phi_j^*(\overline{x}; \overline{\mathbf{R}}) \left(\sum_{l=1}^{N_{\mathrm{N}}} \frac{\nabla_{\mathbf{R}_l}^2}{M_l} \right) \Phi_k(\overline{x}; \overline{\mathbf{R}}) \tag{10.14}$$

are non-adiabatic coupling terms.

The BO approximation consists in neglecting the non-adiabatic coupling terms A_{jk} and B_{jk}. This neglection can be rationalized by (i) the small value of the $1/M_l$ nuclear-mass factors in the expressions (10.13) and (10.14), and (ii) the small value of $\nabla_{\mathbf{R}_l} \Phi_k(\overline{x}; \overline{\mathbf{R}})$, which is assured as long as the electronic states $\Phi_k(\overline{x}; \overline{\mathbf{R}})$ change

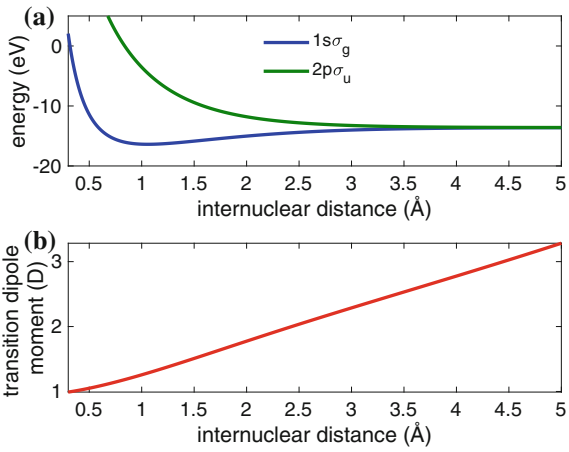

Fig. 10.1 **a** Potential energy curves for the ground and first excited state of H_2^+. **b** Transition dipole moment between the $1s\sigma_g$ state and the $2p\sigma_u$ state

slowly with $\overline{\mathbf{R}}$. If we also neglect the term $U_{\mathrm{N}}(t)$ in (10.10) by considering that it only affects the center-of-mass motion, we arrive at the BO TDSE,

$$\mathrm{i}\hbar\frac{\partial\chi_j(\overline{\mathbf{R}},t)}{\partial t} = \left(T_{\mathrm{N}} + V_j^{\mathrm{BO}}(\overline{\mathbf{R}})\right)\chi_j(\overline{\mathbf{R}},t) - \mathbf{E}(t)\cdot\sum_{k=1}^{L_{\mathrm{BO}}}\boldsymbol{\mu}_{jk}(\overline{\mathbf{R}})\chi_k(\overline{\mathbf{R}},t). \quad (10.15)$$

The physical picture of (10.15) is that each nuclear wave packet $\chi_j(\overline{\mathbf{R}},t)$ moves on a potential energy surface $V_j^{\mathrm{BO}}(\overline{\mathbf{R}})$. Transitions between different electronic states are described by the $\overline{\mathbf{R}}$-dependent transition dipole matrix elements $\boldsymbol{\mu}_{jk}(\overline{\mathbf{R}})$. In Fig. 10.1, we show an example of the BO potential energy curves and transition dipole moment for a hydrogen molecular ion, H_2^+. In H_2^+, there is only one internal nuclear coordinate, the internuclear distance. The potential energy curves shown in Fig. 10.1 were calculated by solving (10.7) with the finite-difference method at each value of the internuclear distance.

It is true that the BH expansion together with the BO approximation works well for many cases of laser-molecule interaction, and is a standard method for the simulation and interpretation of experimental results, but there are of course some limits. We would like to point out a few of the disadvantageous points of the BO approximation, which serve as a motivation for developing methods which go beyond the BO approximation.

(i) The magnitude of the A_{jk} and B_{jk} operators may become unrealistically large at a nuclear geometry $\overline{\mathbf{R}}$ where j-th and k-th BO potential energy surfaces are close in energy to satisfy $\mathscr{E}_j(\overline{\mathbf{R}}) \approx \mathscr{E}_k(\overline{\mathbf{R}})$. By using (10.7), we can derive

$$\int \mathrm{d}\overline{x}\Phi_j^*(\overline{x};\overline{\mathbf{R}})\left(\sum_{l=1}^{N_\mathrm{N}}\frac{\nabla_{\overline{\mathbf{R}}_l}}{M_l}\right)\Phi_k(\overline{x};\overline{\mathbf{R}}) = \frac{\int \mathrm{d}\overline{x}\Phi_j^*(\overline{x};\overline{\mathbf{R}})\left(\sum_{l=1}^{N_\mathrm{N}}\frac{(\nabla_{\overline{\mathbf{R}}_l}H_\mathrm{e})}{M_l}\right)\Phi_k(\overline{x};\overline{\mathbf{R}})}{\mathscr{E}_k(\overline{\mathbf{R}})-\mathscr{E}_j(\overline{\mathbf{R}})}, \tag{10.16}$$

from which it becomes clear that both A_{jk} and B_{jk} become extremely large if $\mathscr{E}_k(\overline{\mathbf{R}}) - \mathscr{E}_j(\overline{\mathbf{R}})$ approaches zero.

(ii) The calculation of potential energy curves is a very difficult task for large molecules. A general, non-linear molecule with N atoms has $3N-6$ vibrational degrees of freedom. If we assume that K points along the coordinate of each vibrational degree of freedom are required for a sufficiently accurate description of the potential energy surface, (10.7) has to be solved K^{3N-6} times, which increases exponentially as N increases. Even for a tetratomic molecule ($N = 4$), we have $3N - 6 = 6$, so that the complete potential energy surface would have to be represented as a 6-dimensional array. Although there are sophisticated methods for fitting high-dimensional potential energy surfaces (see for example [12]), the accurate representation of high-dimensional potential energy surfaces is a difficult problem.

(iii) Omission of electron excitation and ionization. In the BH expansion, we always have to limit the number of electronic states L_BO included in the expansion of the wave function (see (10.8)). Typically, L_BO is set to be $L_\mathrm{BO} < 5$, meaning that only the electronic states with the lowest energy (ground state + a few excited states) are included. Extensive excitation to Rydberg states, doubly excites states, continuum electronic states, which would be required to describe ionization, are difficult to be treated. The omission of such highly excited states and continuum states becomes particularly problematic when we describe the interaction of molecules with ultrashort and intense laser pulses, because ionization and excitation occur with a high probability. In the simplest case of a hydrogen molecule H_2, there exist models by which potential energy curves are calculated for quasi-stable doubly excited electronic states as well as for electronic states corresponding to the ionization [13, 14], but for a general, polyatomic molecule, this approach is not practically applicable.

10.3 Extended Multiconfiguration Time-Dependent Hartree-Fock Method

10.3.1 Basic Concepts

In this section, we describe one promising attempt to go beyond the BO approximation, called the extended multiconfiguration time-dependent Hartree-Fock (Ex-MCTDHF) method [15]. The Ex-MCTDHF method is an extension of the multiconfiguration time-dependent Hartree-Fock (MCTDHF) method for electron dynamics [16, 17] (see also [18] for an overview of the method), which is a natural extension of the multiconfiguration time-dependent Hartree (MCTDH) method for nuclear dynamics [19, 20].

The basic idea of all the methods mentioned above is to introduce time-dependent single-particle (or single-mode) functions for the description of the time-dependent dynamics. This means that each degree of freedom is described by its own time-dependent basis set. In this way, any kind of excitation can be described in a flexible manner.

In the Ex-MCTDHF method, the total time-dependent wave function for both nuclei and electrons is written as

$$\Psi(\overline{\mathbf{R}}, \overline{x}, t) = \sum_{J=1}^{L_\mathrm{e}} \chi_J(\overline{\mathbf{R}}, t) \Phi_J(\overline{x}, t), \tag{10.17}$$

using the same notation for the nuclear and electronic coordinates as adopted in Sect. 10.2. In (10.17), $\chi_J(\overline{\mathbf{R}}, t)$ is a time-dependent nuclear wave function, $\Phi_J(\overline{x}, t)$ is a time-dependent electronic wave function, and L_e is the number of terms included in the wave function expansion. In order to make the total wave function antisymmetrized with respect to an exchange of electrons, $\Phi_J(\overline{x}, t)$ is represented as a Slater determinant, constructed from a set of time-dependent electronic spin-orbitals $\phi_k(x, t)$ $(k = 1, \ldots, K_\mathrm{e})$,

$$\Phi_J(\overline{x}, t) = |\phi_{J_1}(t) \ldots \phi_{J_{N_\mathrm{e}}}(t)|, \tag{10.18}$$

where the label J is a composite index $J = (J_1, \ldots, J_{N_\mathrm{e}})$. We should have at least as many spin-orbitals as the number of electrons in the molecule, that is, $K_\mathrm{e} \geq N_\mathrm{e}$. It is assumed that at all times, the spin-orbitals are orthonormal, $\langle \phi_j(t) | \phi_k(t) \rangle = 0$.

We point out here that the meanings of the electronic wave function $\Phi_J(\overline{x}, t)$ in (10.17) and the electronic wave function $\Phi_j(\overline{x}; \overline{\mathbf{R}})$ in the Born-Huang expansion (10.8) are different. In (10.8), $\Phi_j(\overline{x}; \overline{\mathbf{R}})$ represents an electronic state, an eigenfunction of the electronic Hamiltonian $H_\mathrm{e}(\overline{\mathbf{R}})$ at fixed $\overline{\mathbf{R}}$, which is usually expanded into a linear combination of several Slater determinants, but in (10.17), $\Phi_J(\overline{x}, t)$ is a single, time-dependent Slater determinant.

It is frequently assumed that the same spatial orbitals are used to construct spin-orbitals of both spin types. That is, we assume a set of M_e spatial orbitals $\varphi_k(\mathbf{r}, t)$, $k = 1, \ldots, M_\mathrm{e}$, and construct $K_\mathrm{e} = 2M_\mathrm{e}$ spin-orbitals according to

$$\phi_k(x, t) = \begin{cases} \varphi_k(\mathbf{r}, t)\alpha(s) & \text{if } k \leq M_\mathrm{e}, \\ \varphi_{k-M_\mathrm{e}}(\mathbf{r}, t)\beta(s) & \text{if } k > M_\mathrm{e}. \end{cases} \tag{10.19}$$

In (10.19), $\alpha(s)$ and $\beta(s)$ denote spin-up and spin-down spin functions, respectively. In this case, each Slater determinant is labeled by a double index $J = (J^\alpha, J^\beta)$, with $J^\alpha = (J_1^\alpha, \ldots, J_{N_\mathrm{e}^\alpha}^\alpha)$ and $J^\beta = (J_1^\beta, \ldots, J_{N_\mathrm{e}^\beta}^\beta)$. The numbers N_e^α of α electrons and N_e^β of β electrons satisfy $N_\mathrm{e}^\alpha + N_\mathrm{e}^\beta = N_\mathrm{e}$, and we assume that all Slater determinants have the same value of N_e^α and N_e^β. A determinant is written as

$$\Phi_J(\overline{x},t) = |\varphi_{J_1^\alpha}(t)\alpha \ldots \varphi_{J_{N_e^\alpha}^\alpha}(t)\alpha\, \varphi_{J_1^\beta}(t)\beta \ldots \varphi_{J_{N_e^\beta}^\beta}(t)\beta|. \tag{10.20}$$

The total number of electronic Slater determinants that can be constructed in this way is $L_e = \binom{M_e}{N_e^\alpha}\binom{M_e}{N_e^\beta} = M_e!^2/[N_e^\alpha! N_e^\beta! (M_e - N_e^\alpha)!(M_e - N_e^\beta)!]$.

The wave function defined by (10.17) looks very similar to the BO wave function in (10.8). The important difference is that the electronic wave function $\Phi_J(\overline{x},t)$ in (10.17) does not depend on the nuclear coordinates $\overline{\mathbf{R}}$, but instead depends on time t. This means that each electronic wave function $\Phi_J(\overline{x},t)$ is no longer associated with a certain electronic state with a certain energy. At some moment in time, $\Phi_J(\overline{x},t)$ may be a superposition of a bound part (consisting of both ground-state and excited-state components) and a continuum part. This feature makes it possible for a wave function of the type (10.17) to describe arbitrary electronic excitation, including ionization, with a limited number of terms L_e in the sum over J in (10.17). Moreover, because the electronic wave functions do not depend on $\overline{\mathbf{R}}$, there is no need to calculate potential energy surfaces in the Ex-MCTDHF method. The major drawback of an ansatz like the one in (10.17) is that the equations governing the time-evolution of the time-dependent orbitals become non-linear, as we will see below in (10.31), (10.46), and (10.54).

In [15], the ansatz (10.17) was further adapted to describe "diatomic-like" molecules, which refers to molecules consisting of two heavy atoms like O or C and N_p light hydrogen atoms. Explicit examples are C_2H_2 and CH_3OH. The idea proposed in [15] was that the protonic part of the wave function can be expanded in terms of Slater determinants, because protons are also fermions whose wave function needs to be properly antisymmetrized. The motivation of using Slater determinants also for the description of the protonic motion is to make the structure of the wave function as flexible as possible, which can allow us to simulate highly distorted molecular structures such as those appearing in the course of hydrogen migration.

In order to describe the protonic part of the wave function with Slater determinants, the wave function $\chi_J(\overline{\mathbf{R}},t)$ for the nuclear coordinate is expanded as

$$\chi_J(\overline{\mathbf{R}},t) = \sum_{I=1}^{L_p} C_{IJ}(\overline{\mathbf{R}}_h,t)\Lambda_I(\overline{X},t), \tag{10.21}$$

where $\overline{\mathbf{R}}_h$ is the collective coordinate for the two heavy atoms, $\overline{X}$ is the collective spatial-spin coordinate for the N_p protons, and L_p is the number of terms included in the expansion of the nuclear wave function. The proton coordinate $\overline{X}$ is defined as $\overline{X} = (X_1, \ldots, X_{N_p})$ with $X_k = (\mathbf{R}_{pk}, S_k)$ expressed in terms of the spatial coordinate $\mathbf{R}_{pk}$ and the spin coordinate S_k of the proton k. Similarly to the electronic part of the wave function, $\Lambda_I(\overline{X},t)$ is taken to be a Slater determinant constructed from the time-dependent protonic orbitals $\lambda_i(X,t)$,

$$\Lambda_I(\overline{X},t) = |\lambda_{I_1}(t)\ldots\lambda_{I_{N_p}}(t)|, \tag{10.22}$$

with $I = (I_1, \ldots, I_{N_\mathrm{p}})$. In the same way as for the electronic Slater determinants, it is convenient to assume that the same spatial orbitals are used both for α and β spin-orbitals, that is,

$$\lambda_j(X,t) = \begin{cases} \kappa_j(\mathbf{R},t)\alpha(S) & \text{if } j \le M_\mathrm{p}, \\ \kappa_{j-M_\mathrm{p}}(\mathbf{R},t)\beta(S) & \text{if } j > M_\mathrm{p}, \end{cases} \tag{10.23}$$

where we have assumed that there are M_p spatial protonic orbitals. The protonic Slater determinants are in this case written as

$$\Lambda_I(\overline{X},t) = |\kappa_{I_1^\alpha}(t)\alpha \ldots \kappa_{I_{N_\mathrm{p}^\alpha}^\alpha}(t)\alpha\, \kappa_{I_1^\beta}(t)\beta \ldots \kappa_{I_{N_\mathrm{p}^\beta}^\beta}(t)\beta|, \tag{10.24}$$

where there are N_p^α α-spin protons and N_p^β β-spin protons in each determinant. The total number of protons is $N_\mathrm{p} = N_\mathrm{p}^\alpha + N_\mathrm{p}^\beta$. Similarly to the electronic determinants, we have a total number of $L_\mathrm{p} = \binom{M_\mathrm{p}}{N_\mathrm{p}^\alpha}\binom{M_\mathrm{p}}{N_\mathrm{p}^\beta} = M_\mathrm{p}!^2/[N_\mathrm{p}^\alpha!N_\mathrm{p}^\beta!(M_\mathrm{p}-N_\mathrm{p}^\alpha)!(M_\mathrm{p}-N_\mathrm{p}^\beta)!]$ protonic Slater determinants.

Substituting (10.21) into (10.17), we find for the total wave function,

$$\Psi(\overline{\mathbf{R}}_\mathrm{h}, \overline{X}, \overline{x}, t) = \sum_{J=1}^{L_\mathrm{e}} \sum_{I=1}^{L_\mathrm{p}} C_{IJ}(\overline{\mathbf{R}}_\mathrm{h}, t)\Lambda_I(\overline{X}, t)\Phi_J(\overline{x}, t). \tag{10.25}$$

Due to the similarity of (10.25) to the configuration-interaction expansion of a many-electron wave function [21], we refer to the $C_{IJ}(\overline{\mathbf{R}}_\mathrm{h}, t)$ as time-dependent configuration-interaction (CI) coefficients.

Because all factors $[C_{IJ}(\overline{\mathbf{R}}_\mathrm{h}, t)$, $\Lambda_I(\overline{X}, t)$, and $\Phi_J(\overline{x}, t)]$ depend on t, we have to derive appropriate evolution equations. In order to derive the evolution equations, also referred to as the equations of motion, we employ the time-dependent variational principle [22, 23],

$$\langle \delta\Psi(t)|H - \mathrm{i}\hbar\frac{\partial}{\partial t}|\Psi(t)\rangle = 0, \tag{10.26}$$

where $\delta\Psi(t)$ is the variation of the total wave function with respect to parameters $C_{IJ}(\overline{\mathbf{R}}_\mathrm{h}, t)$, $\Lambda_I(\overline{X}, t)$, and $\Phi_J(\overline{x}, t)$, and the bra-ket in (10.26) implies the integration over all variables $\overline{\mathbf{R}}_\mathrm{h}$, $\overline{X}$, and $\overline{x}$. Orthogonality of the electronic and protonic orbitals, $\langle\varphi_j(t)|\varphi_k(t)\rangle = \langle\kappa_j(t)|\kappa_k(t)\rangle = \delta_{jk}$, is assumed by introducing suitable Lagrange multipliers in (10.26).

Before we derive the equations of motion for the Ex-MCTDHF method, we first define the single-proton Hamiltonian,

$$h_\mathrm{p}(\mathbf{R},t) = -\frac{\hbar^2}{2m_\mathrm{p}}\nabla_\mathbf{R}^2 - e\mathbf{E}(t)\cdot\mathbf{R}, \tag{10.27}$$

where m_p is the mass of the proton, the single-electron Hamiltonian,

$$h_{\mathrm{e}}(\mathbf{r},t) = -\frac{\hbar^2}{2m_{\mathrm{e}}}\nabla_{\mathbf{r}}^2 + e\mathbf{E}(t)\cdot\mathbf{r}, \tag{10.28}$$

and the Hamiltonian for the $N_{\mathrm{h}} = N_{\mathrm{N}} - N_{\mathrm{p}}$ heavy particles,

$$H_{\mathrm{h}}(\overline{\mathbf{R}}_{\mathrm{h}},t) = \sum_{k=1}^{N_{\mathrm{h}}}\left(-\frac{\hbar^2}{2M_k}\nabla_{\mathbf{R}_{\mathrm{h}k}}^2 - e\mathbf{E}(t)\cdot\mathbf{R}_{\mathrm{h}k} + \sum_{l<k}\frac{Z_l Z_k e^2}{4\pi\varepsilon_0|\mathbf{R}_{\mathrm{h}k}-\mathbf{R}_{\mathrm{h}l}|}\right), \tag{10.29}$$

where Z_k here represents the charge number of the heavy nucleus k. In [15], it was assumed that $N_{\mathrm{h}} = 2$. Then, the total Hamiltonian can now be written as

$$\begin{aligned} H = &\sum_{k=1}^{N_{\mathrm{p}}} h_{\mathrm{p}}(\mathbf{R}_{\mathrm{p}k},t) + \sum_{k=1}^{N_{\mathrm{p}}}\sum_{l<k}\frac{e^2}{4\pi\varepsilon_0|\mathbf{R}_{\mathrm{p}k}-\mathbf{R}_{\mathrm{p}l}|} \\ &+ \sum_{k=1}^{N_{\mathrm{e}}} h_{\mathrm{e}}(\mathbf{r}_k,t) + \sum_{k=1}^{N_{\mathrm{e}}}\sum_{l<k}\frac{e^2}{4\pi\varepsilon_0|\mathbf{r}_k-\mathbf{r}_l|} \\ &- \sum_{k=1}^{N_{\mathrm{p}}}\sum_{l=1}^{N_{\mathrm{e}}}\frac{e^2}{4\pi\varepsilon_0|\mathbf{R}_{\mathrm{p}k}-\mathbf{r}_l|} - \sum_{k=1}^{N_{\mathrm{h}}}\sum_{l=1}^{N_{\mathrm{e}}}\frac{Z_k e^2}{4\pi\varepsilon_0|\mathbf{R}_{\mathrm{h}k}-\mathbf{r}_l|} + \sum_{k=1}^{N_{\mathrm{h}}}\sum_{l=1}^{N_{\mathrm{p}}}\frac{Z_k e^2}{4\pi\varepsilon_0|\mathbf{R}_{\mathrm{h}k}-\mathbf{R}_{\mathrm{p}l}|} \\ &+ H_{\mathrm{h}}(\overline{\mathbf{R}}_{\mathrm{h}},t). \end{aligned} \tag{10.30}$$

We note that the Hamiltonian (10.30) is the same as that in (10.1), but the form is rewritten so that the different interaction terms appear more clearly.

10.3.2 Equations of Motion

In order to obtain the equation of motion for the electronic orbitals, we take the variation $\delta\Psi$ with respect to one spatial orbital φ_k in (10.26). The result is

$$\begin{aligned} \mathrm{i}\hbar\frac{\partial\varphi_k(\mathbf{r},t)}{\partial t} = Q_{\mathrm{e}}(t)\sum_{lm} D_{kl}^{\mathrm{e}-1}(t)\Big(&D_{lm}^{\mathrm{e}}(t)h_{\mathrm{e}}(\mathbf{r},t) + W_{lm}^{\mathrm{ee}}(\mathbf{r},t) + W_{lm}^{\mathrm{ep}}(\mathbf{r},t) \\ &+ W_{lm}^{\mathrm{eh}}(\mathbf{r},t)\Big)\varphi_m(\mathbf{r},t), \end{aligned} \tag{10.31}$$

where

$$D_{lm}^{\mathrm{e}}(t) = \sum_{IPQ}\int \mathrm{d}\overline{\mathbf{R}}_{\mathrm{h}} C_{IP}^*(\overline{\mathbf{R}}_{\mathrm{h}},t)C_{IQ}(\overline{\mathbf{R}}_{\mathrm{h}},t)\mathscr{O}_{PQlm}^{\mathrm{e}} \tag{10.32}$$

is the spin-summed electronic first-order density matrix,

$$W^{\mathrm{ee}}_{lm}(\mathbf{r},t) = \sum_{pq} d^{\mathrm{e}}_{lmpq}(t) g^{\mathrm{ee}}_{pq}(\mathbf{r},t) \tag{10.33}$$

is the electron-electron interaction defined using the spin-summed electronic second-order density matrix,

$$d^{\mathrm{e}}_{klmn}(t) = \sum_{IPQ} \int \mathrm{d}\overline{\mathbf{R}}_{\mathrm{h}} C^{*}_{IP}(\overline{\mathbf{R}}_{\mathrm{h}},t) C_{IQ}(\overline{\mathbf{R}}_{\mathrm{h}},t) \mathscr{F}^{\mathrm{e}}_{PQklmn}, \tag{10.34}$$

and the repulsive electron-electron Coulomb potential

$$g^{\mathrm{ee}}_{pq}(\mathbf{r},t) = \frac{e^2}{4\pi\varepsilon_0} \int \mathrm{d}\mathbf{r}' \frac{\varphi^{*}_{p}(\mathbf{r}',t)\varphi_q(\mathbf{r}',t)}{|\mathbf{r}-\mathbf{r}'|}, \tag{10.35}$$

the electron-proton interaction is

$$W^{\mathrm{ep}}_{lm}(\mathbf{r},t) = \sum_{IJPQrs} \int \mathrm{d}\overline{\mathbf{R}}_{\mathrm{h}} C^{*}_{IP}(\overline{\mathbf{R}}_{\mathrm{h}},t) C_{JQ}(\overline{\mathbf{R}}_{\mathrm{h}},t) \mathscr{O}^{\mathrm{e}}_{PQlm} \mathscr{O}^{\mathrm{p}}_{IJrs} g^{\mathrm{ep}}_{rs}(\mathbf{r},t) \tag{10.36}$$

defined with the attractive electron-proton Coulomb potential

$$g^{\mathrm{ep}}_{pq}(\mathbf{r},t) = -\frac{e^2}{4\pi\varepsilon_0} \int \mathrm{d}\mathbf{R} \frac{\kappa^{*}_{p}(\mathbf{R},t)\kappa_q(\mathbf{R},t)}{|\mathbf{r}-\mathbf{R}|}, \tag{10.37}$$

and the attractive electron-heavy nuclei interaction is

$$W^{\mathrm{eh}}_{lm}(\mathbf{r},t) = -\frac{e^2}{4\pi\varepsilon_0} \sum_{IPQ} \mathscr{O}^{\mathrm{e}}_{PQlm} \int \mathrm{d}\overline{\mathbf{R}}_{\mathrm{h}} C^{*}_{IP}(\overline{\mathbf{R}}_{\mathrm{h}},t) C_{IQ}(\overline{\mathbf{R}}_{\mathrm{h}},t) \left(\sum_{k=1}^{N_{\mathrm{h}}} \frac{Z_k}{|\mathbf{R}_{\mathrm{h}k}-\mathbf{r}|} \right). \tag{10.38}$$

In (10.32), (10.34), (10.36) and (10.38), we have used the following matrix elements of the spin-summed excitation operators $\hat{\mathscr{E}}_{pq}$ and $\hat{\mathscr{F}}_{pqrs}$ [21],

$$\mathscr{O}^{\mathrm{e}}_{PQlm} = \langle \Phi_P(t) | \hat{\mathscr{E}}_{lm} | \Phi_Q(t) \rangle, \tag{10.39}$$

$$\mathscr{O}^{\mathrm{p}}_{IJrs} = \langle \Lambda_I(t) | \hat{\mathscr{E}}_{rs} | \Lambda_J(t) \rangle, \tag{10.40}$$

and

$$\mathscr{F}^{\mathrm{e}}_{PQklmn} = \langle \Phi_P(t) | \hat{\mathscr{F}}_{klmn} | \Phi_Q(t) \rangle. \tag{10.41}$$

For later use, we additionally define

$$\mathscr{F}^{\mathrm{p}}_{IJklmn} = \langle \Lambda_I(t) | \hat{\mathscr{F}}_{klmn} | \Lambda_J(t) \rangle. \tag{10.42}$$

The spin-summed excitation operators are defined using the creation and annihilation operators $\hat{a}^\dagger_{p\sigma}$ and $\hat{a}_{q\sigma}$ as [21]

$$\hat{\mathscr{E}}_{pq} = \sum_{\sigma=\alpha,\beta} \hat{a}^\dagger_{p\sigma}\hat{a}_{q\sigma} \tag{10.43}$$

and

$$\hat{\mathscr{F}}_{pqrs} = \hat{\mathscr{E}}_{pq}\hat{\mathscr{E}}_{rs} - \delta_{qr}\hat{\mathscr{E}}_{ps}. \tag{10.44}$$

Upon the operation of the creation operator $\hat{a}^\dagger_{p\sigma}$ on a Slater determinant (either electronic or protonic), the spatial orbital p with spin σ (=α or β) is created. On the other hand, upon the operation of the annihilation operator $\hat{a}_{q\sigma}$, the spatial orbital q with spin σ is annihilated if it exists in the determinant. The matrix elements defined in (10.39)–(10.42) are equal to either 0, −1, or 1. We can derive their explicit values for different combinations of indexes by using the orthonormality of the spatial orbitals and by taking into account the sign change of a determinant upon the permutation of the order of the orbitals. The matrix elements, $\mathscr{E}^{\mathrm{e}}_{PQlm}$ and $\mathscr{E}^{\mathrm{p}}_{PQlm}$, can take non-zero values only when the two determinants involved differ by at most one orbitals, and the matrix elements, $\mathscr{F}^{\mathrm{e}}_{PQklmn}$ and $\mathscr{F}^{\mathrm{p}}_{PQklmn}$, are non-zero only when the two determinants differ by at most two orbitals. We also note that $\mathscr{E}^{\mathrm{e}}_{PQlm}$, $\mathscr{E}^{\mathrm{p}}_{PQlm}$, $\mathscr{F}^{\mathrm{e}}_{PQklmn}$ and $\mathscr{F}^{\mathrm{p}}_{PQklmn}$ defined (in (10.39)–(10.42)) as matrix elements composed of time-dependent determinants, are independent of time.

The symbol Q_{e} in the equation of motion (10.31) is a projection operator whose action on an arbitrary function $f(\mathbf{r})$ is defined as

$$Q_{\mathrm{e}}(t)f(\mathbf{r}) = f(\mathbf{r}) - \sum_k f(\mathbf{r})\langle f|\varphi_k(t)\rangle. \tag{10.45}$$

The projection operator $Q_{\mathrm{e}}(t)$ appears in the equation of motion (10.31) because of the restriction of $\langle\varphi_j(t)|\varphi_k(t)\rangle = \delta_{jk}$ imposed by the Lagrange multipliers. By multiplying the equation of motion (10.31) by $\varphi^*_j(\mathbf{r},t)$ and integrating over $\mathbf{r}$, we may confirm that $\langle\varphi_j|(\partial/\partial t)|\varphi_k\rangle = 0$ holds for arbitrary j and k if $\langle\varphi_j(t)|\varphi_k(t)\rangle = \delta_{jk}$ because of the presence of $Q_{\mathrm{e}}(t)$, and therefore, $\langle\varphi_j(t)|\varphi_k(t)\rangle = \delta_{jk}$ is satisfied for all t provided that the orbital set $\{\varphi_j(t)\}$ is orthonormal at $t = 0$.

The equation of motion for the protonic orbitals $\kappa_j(\mathbf{R},t)$ is calculated by taking the variation $\delta\Psi$ in (10.26) with respect to κ_j on the condition that $\langle\kappa_j(t)|\kappa_k(t)\rangle = \delta_{jk}$. We obtain the following equation of motion, similar to that for the electronic orbitals, (10.31),

$$\mathrm{i}\hbar\frac{\partial\kappa_k(\mathbf{R},t)}{\partial t} = Q_{\mathrm{p}}(t)\sum_{lm} D^{\mathrm{p}-1}_{kl}(t)\Big(D^{\mathrm{p}}_{lm}(t)h_{\mathrm{p}}(\mathbf{R},t) + W^{\mathrm{pp}}_{lm}(\mathbf{R},t) + W^{\mathrm{pe}}_{lm}(\mathbf{R},t) + W^{\mathrm{ph}}_{lm}(\mathbf{R},t)\Big)\kappa_m(\mathbf{R},t), \tag{10.46}$$

where

$$D^{\mathrm{p}}_{lm}(t) = \sum_{IJP} \int \mathrm{d}\overline{\mathbf{R}}_{\mathrm{h}} C^{*}_{IP}(\overline{\mathbf{R}}_{\mathrm{h}}, t) C_{JP}(\overline{\mathbf{R}}_{\mathrm{h}}, t) \mathscr{O}^{\mathrm{p}}_{IJlm} \tag{10.47}$$

is the spin-summed protonic first-order density matrix,

$$W^{\mathrm{pp}}_{lm}(\mathbf{R}, t) = \sum_{pq} d^{\mathrm{p}}_{lmpq}(t) g^{\mathrm{pp}}_{pq}(\mathbf{R}, t) \tag{10.48}$$

is the proton-proton interaction with the spin-summed protonic second-order density matrix,

$$d^{\mathrm{p}}_{klmn}(t) = \sum_{IJP} \int \mathrm{d}\overline{\mathbf{R}}_{\mathrm{h}} C^{*}_{IP}(\overline{\mathbf{R}}_{\mathrm{h}}, t) C_{JP}(\overline{\mathbf{R}}_{\mathrm{h}}, t) \mathscr{F}^{\mathrm{p}}_{IJklmn}, \tag{10.49}$$

and the proton-proton Coulomb potential,

$$g^{\mathrm{pp}}_{pq}(\mathbf{R}, t) = \frac{e^2}{4\pi\varepsilon_0} \int \mathrm{d}\mathbf{R}' \frac{\kappa^{*}_{p}(\mathbf{R}', t)\kappa_q(\mathbf{R}', t)}{|\mathbf{R} - \mathbf{R}'|}. \tag{10.50}$$

Furthermore,

$$W^{\mathrm{pe}}_{lm}(\mathbf{R}, t) = \sum_{IJPQrs} \int \mathrm{d}\overline{\mathbf{R}}_{\mathrm{h}} C^{*}_{IP}(\overline{\mathbf{R}}_{\mathrm{h}}, t) C_{JQ}(\overline{\mathbf{R}}_{\mathrm{h}}, t) \mathscr{O}^{\mathrm{e}}_{PQlm} \mathscr{O}^{\mathrm{p}}_{IJrs} g^{\mathrm{pe}}_{rs}(\mathbf{R}, t) \tag{10.51}$$

is the proton-electron interaction defined using the attractive proton-electron Coulomb potential,

$$g^{\mathrm{pe}}_{pq}(\mathbf{R}, t) = -\frac{e^2}{4\pi\varepsilon_0} \int \mathrm{d}\mathbf{r} \frac{\varphi^{*}_{p}(\mathbf{r}, t)\varphi_q(\mathbf{r}, t)}{|\mathbf{r} - \mathbf{R}|}, \tag{10.52}$$

and

$$W^{\mathrm{ph}}_{lm}(\mathbf{R}, t) = \frac{e^2}{4\pi\varepsilon_0} \sum_{IJP} \mathscr{O}^{\mathrm{p}}_{IJlm} \int \mathrm{d}\overline{\mathbf{R}}_{\mathrm{h}} C^{*}_{IP}(\overline{\mathbf{R}}_{\mathrm{h}}, t) C_{JP}(\overline{\mathbf{R}}_{\mathrm{h}}, t) \left(\sum_{k=1}^{N_{\mathrm{h}}} \frac{Z_k}{|\mathbf{R}_{\mathrm{h}k} - \mathbf{R}|} \right) \tag{10.53}$$

is the repulsive proton-heavy nuclei interaction.

Finally, we take the variation with respect to the coefficients $C_{IJ}(\overline{\mathbf{R}}_{\mathrm{h}}, t)$, which results in the equation of motion,

$$\begin{aligned} \mathrm{i}\hbar \frac{\partial C_{IJ}(\overline{\mathbf{R}}_{\mathrm{h}}, t)}{\partial t} &= H_{\mathrm{h}}(\overline{\mathbf{R}}_{\mathrm{h}}, t) C_{IJ}(\overline{\mathbf{R}}_{\mathrm{h}}, t) \\ &\quad + \sum_{KL} \left(W^{\mathrm{he}}_{IJKL}(\overline{\mathbf{R}}_{\mathrm{h}}, t) + W^{\mathrm{hp}}_{IJKL}(\overline{\mathbf{R}}_{\mathrm{h}}, t) + W^{0}_{IJKL}(t) \right) C_{KL}(\overline{\mathbf{R}}_{\mathrm{h}}, t). \end{aligned} \tag{10.54}$$

In (10.54), $H_{\rm h}(\overline{\mathbf{R}}_{\rm h}, t)$ is given by (10.29),

$$W^{\rm he}_{IJKL}(\overline{\mathbf{R}}_{\rm h}, t) = -\delta_{IK}\frac{e^2}{4\pi\varepsilon_0}\sum_{lm}\mathscr{E}^{\rm e}_{JLlm}\left(\sum_{k=1}^{N_{\rm h}} Z_k \int {\rm d}\mathbf{r}\frac{\varphi^*_l(\mathbf{r}, t)\varphi_m(\mathbf{r}, t)}{|\mathbf{R}_{{\rm h}k} - \mathbf{r}|}\right) \tag{10.55}$$

is the heavy nuclei-electron interaction,

$$W^{\rm hp}_{IJKL}(\overline{\mathbf{R}}_{\rm h}, t) = \delta_{JL}\frac{e^2}{4\pi\varepsilon_0}\sum_{lm}\mathscr{E}^{\rm p}_{IKlm}\left(\sum_{k=1}^{N_{\rm h}} Z_k \int {\rm d}\mathbf{R}\frac{\kappa^*_l(\mathbf{R}, t)\kappa_m(\mathbf{R}, t)}{|\mathbf{R}_{{\rm h}k} - \mathbf{R}|}\right) \tag{10.56}$$

is the heavy nuclei-proton interaction, and

$$\begin{aligned} W^0_{IJKL}(t) = {} & \delta_{IK}\left(\sum_{kl}\mathscr{E}^{\rm e}_{JLkl}\langle\varphi_k(t)|h_{\rm e}(t)|\varphi_l(t)\rangle + \frac{1}{2}\sum_{klmn}\mathscr{F}^{\rm e}_{JLklmn}\langle\varphi_m(t)|g^{\rm ee}_{kl}(t)|\varphi_n(t)\rangle\right) \\ & + \delta_{JL}\left(\sum_{kl}\mathscr{E}^{\rm p}_{IKkl}\langle\kappa_k(t)|h_{\rm p}(t)|\kappa_l(t)\rangle + \frac{1}{2}\sum_{klmn}\mathscr{F}^{\rm p}_{IKklmn}\langle\kappa_m(t)|g^{\rm pp}_{kl}(t)|\kappa_n(t)\rangle\right) \\ & + \sum_{lmrs}\mathscr{E}^{\rm e}_{JLlm}\mathscr{E}^{\rm p}_{IKrs}\langle\varphi_l(t)|g^{\rm ep}_{rs}(t)|\varphi_m(t)\rangle \end{aligned} \tag{10.57}$$

is an $\overline{\mathbf{R}}_{\rm h}$-independent matrix. The CI coefficients $C_{IJ}(\overline{\mathbf{R}}_{\rm h}, t)$ are not orthonormal in general, that is, $\int {\rm d}\overline{\mathbf{R}}_{\rm h} C^*_{IJ}(\overline{\mathbf{R}}_{\rm h}, t)C_{KL}(\overline{\mathbf{R}}_{\rm h}, t) \neq 0$ for $IJ \neq KL$. However, the total wave function is normalized as

$$\sum_{I=1}^{L_{\rm e}}\sum_{J=1}^{L_{\rm p}}\int {\rm d}\overline{\mathbf{R}}_{\rm h} C^*_{IJ}(\overline{\mathbf{R}}_{\rm h}, t)C_{IJ}(\overline{\mathbf{R}}_{\rm h}, t) = 1. \tag{10.58}$$

We remark here that the equations of motion (10.31), (10.46), and (10.54) presented above are the same as those given in the original publication [15] even though the notations are different.

The interaction potentials W^{xy}_{lm} (where $x, y = {\rm e}, {\rm p}, {\rm h}$) in general arise from the inter-particle Coulomb potentials (repulsive or attractive), but the Coulomb potentials always appear as those averaged over the particle distributions. For example, in the case of the electron-proton interaction term $W^{\rm ep}_{lm}(\mathbf{r}, t)$ defined in (10.36), the Coulomb potential $g^{\rm ep}_{pq}(\mathbf{r}, t)$ (defined in (10.37)) is not the bare Coulomb potential $-e^2/(4\pi\varepsilon_0|\mathbf{r} - \mathbf{R}|)$, but is that averaged over the protonic orbitals $\kappa_p(\mathbf{R}, t)$ and $\kappa_q(\mathbf{R}, t)$.

Even though we have presented the general equations of motion for $\overline{\mathbf{R}}_{\rm h}$-dependent CI coefficients as seen in (10.54), we can assume that the heavy nuclei, i. e., all nuclei except for the protons, in the molecule are immobile, which corresponds to the clamped-nuclei approximation. In this case, the coordinates of the heavy nuclei should be treated as a parameter, and the heavy-nuclei Hamiltonian $H_{\rm h}(\overline{\mathbf{R}}_{\rm h}, t)$

in (10.30) should be omitted. As a result, the first line of (10.54) involving the term $H_{\rm h}(\overline{\mathbf{R}}_{\rm h}, t)C_{IJ}(\overline{\mathbf{R}}_{\rm h}, t)$ disappears, and the equation of motion for the CI coefficients becomes an ordinary differential equation (in t) instead of a partial differential equation. Moreover, all integrations over the heavy nuclei coordinates $\overline{\mathbf{R}}_{\rm h}$ should be dropped, so that the electron-heavy nuclei potential (10.38) and the proton-heavy-nuclei potential (10.53) depend on a parameter $\overline{\mathbf{R}}_{\rm h}$.

We can find the ground state wave function, that is, the Ex-MCTDHF wave function Ψ that minimizes the total energy $\mathscr{E} = \langle\Psi|H|\Psi\rangle$, by integrating the equations of motion (10.31), (10.46), and (10.54) in imaginary time [17]. This means that the time t is replaced by $-i\tau$, resulting in $i\partial/\partial t \rightarrow -\partial/\partial\tau$, so that the TDSE takes the form of a diffusion equation.

10.3.3 Applications of the Ex-MCTDHF Method

Thus far, only two reports [24, 25] have been published on the application of the Ex-MCTDHF method. Both of these applications deal with the stationary properties of ground-state wave functions. The equations of motion derived in the preceding Sect. 10.3.2 are used in this section to obtain the optimal ground state via the imaginary time propagation.

10.3.3.1 CH_3OH

In [24], the Ex-MCTDHF method was applied to the calculation of the electro-protonic ground state wave function of methanol, CH_3OH. The oxygen atom and the carbon atom were treated as heavy nuclei, and rotation of the molecule was neglected, which means that $\overline{\mathbf{R}}_{\rm h} = R_{\rm CO}$, the C–O internuclear distance. Furthermore, the clamped nuclei approximation was assumed for C and O, so that $R_{\rm CO}$ was treated as a parameter. Since the C atom and the O atom define a molecular axis, and the total Hamiltonian for the electrons and the protons is symmetric under rotations around this axis, cylindrical symmetry around the C–O axis can be assumed for the electronic and protonic orbitals. If we take the C–O axis to be the z-axis in the cylindrical coordinate system, we have $\mathbf{r}_k = (z_{{\rm e}k}, \rho_{{\rm e}k}, \phi_{{\rm e}k})$ for the coordinate of the electron k, and $\mathbf{R}_{{\rm p}l} = (z_{{\rm p}l}, \rho_{{\rm p}l}, \phi_{{\rm p}l})$ for the coordinate of the proton l. We have

$$\varphi_k(\mathbf{r}_{\rm e}, t) = f_k(z_{\rm e}, \rho_{\rm e}, t)\mathrm{e}^{\mathrm{i}m_{{\rm e}k}\phi_{\rm e}} \tag{10.59}$$

for the electronic spatial orbitals, and

$$\kappa_k(\mathbf{R}_{\rm p}, t) = g_k(z_{\rm p}, \rho_{\rm p}, t)\mathrm{e}^{\mathrm{i}m_{{\rm p}k}\phi_{\rm p}} \tag{10.60}$$

for the protonic spatial orbitals. Both the electronic orbitals and the protonic orbitals were discretized using the grid method. In (10.59) and (10.60), the quantum numbers

m_{ek} and m_{pk} determine the angular momentum around the molecular axis of the respective orbital. In [24], the values $|m_{ek}| \leq 1$ and $|m_{pk}| \leq 3$ were adopted. For the electronic structure, a single closed-shell Slater determinant was adopted, meaning that $L_e = 1$ in (10.25). For the protonic wave function, a total of $M_p = 16$ spatial orbitals were employed, and determinants with the highest possible protonic spin, $S = 2$, were constructed. This means that $N_p^\alpha = 4$ and $N_p^\beta = 0$ in (10.24), and $L_p = \binom{16}{4} = 1820$ in (10.25).

The main result obtained in [24] is that the molecular structure of a polyatomic molecule such as CH_3OH in the absence of a laser field can indeed be described by the Ex-MCTDHF ansatz given in (10.25). This is a remarkable result, because the spatial distribution of the protons is not determined from the energy minimum of a potential energy surface, but is the result of the optimization of the Ex-MCTDHF ground state wave function.

The protonic structure of CH_3OH was elucidated first by calculating the 2-proton spatial distribution,

$$\Gamma_p(\mathbf{R}_{p1}, \mathbf{R}_{p2}) = \frac{1}{2} \sum_{klmn} d^p_{klmn} \kappa^*_k(\mathbf{R}_{p1}) \kappa_l(\mathbf{R}_{p1}) \kappa^*_m(\mathbf{R}_{p2}) \kappa_n(\mathbf{R}_{p2}), \tag{10.61}$$

expressed in terms of the spin-summed protonic second-order density matrix d^p_{klmn} defined in (10.49). $\Gamma_p(\mathbf{R}_{p1}, \mathbf{R}_{p2})$ represents the probability distribution of finding one proton at $\mathbf{R}_{p1}$ and another one at $\mathbf{R}_{p2}$. We can now define a conditional 1-proton distribution $D_p(\mathbf{R}_p|\mathbf{R}_0) = \Gamma_p(\mathbf{R}_p, \mathbf{R}_0)$ by fixing one of the proton positions in $\Gamma_p(\mathbf{R}_{p1}, \mathbf{R}_{p2})$ to $\mathbf{R}_0$. $D_p(\mathbf{R}_p|\mathbf{R}_0)$ represents the spatial proton distribution of the three remaining protons, given that the position of the fourth proton is fixed to $\mathbf{R}_0$.

In Fig. 10.2, we show the conditional 1-proton distribution $D_p(x_p, y_p|\mathbf{R}_0) = \int dz_p D_p(\mathbf{R}_p|\mathbf{R}_0)$ in the xy-plane, integrated along the z-axis (the C–O axis). The fixed position $\mathbf{R}_0$ of one of the protons is taken to be the most probable position of the proton in the hydroxyl group, $\mathbf{R}_0 = (z_0, \rho_0, \phi_0) = (-2.02\, a_0, 1.78\, a_0, 0)$, where $a_0 \approx 0.53$ Å denotes Bohr's radius. As expected, the proton distribution in the xy-plane exhibits three maxima, consistent with the protonic structure of the methyl group in CH_3OH. For comparison, we also show in Fig. 10.2 the conventional ball-and-stick representation of CH_3OH, corresponding to the positions of the nuclei yielding the lowest total energy on the BO potential energy surface.

The results presented in [24] show that the spatial correlation among protons in a molecule containing several protons can be correctly reproduced with an Ex-MCTDHF wave function, provided that the number of protonic orbitals included in the wave function expansion is sufficiently large. It was shown in [24] that the spatial correlations among the four protons in CH_3OH were properly described when $M_p = 16$ and $|m_{pk}| \leq 3$ as shown in Fig. 10.2a, and that the three distinct peaks seen in Fig. 10.2a, corresponding to the methyl-group protons, were not reproduced when a smaller set of $M_p = 12$ protonic orbitals including orbital angular momentum $|m_{pk}| \leq 2$ was adopted.

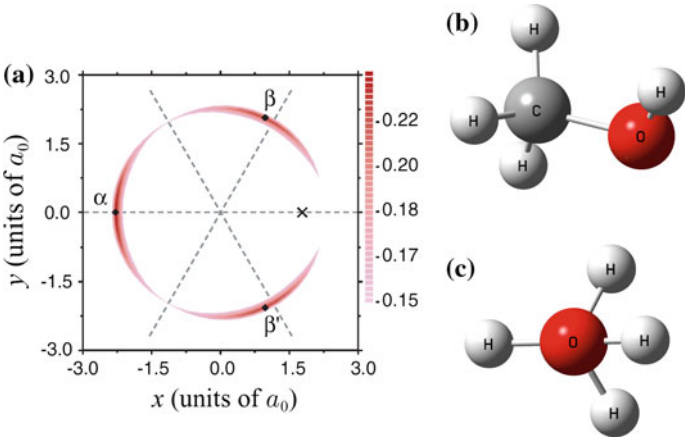

Fig. 10.2 **a** Conditional probability distribution $D_{\mathrm{p}}(x_{\mathrm{p}}, y_{\mathrm{p}}|\mathbf{R}_0)$, taken from [24]. One proton is fixed at the point marked with a cross ×, corresponding to the most probable position of the proton in the OH group. The peaks in the distribution labeled with α, β, and β′ correspond to the protons in the methyl group on the side of the C atom. **b** Ball-and-stick model of CH_3OH. The C–O axis defines the z-axis, while the xy-plane is perpendicular to the C–O axis. **c** Ball-and-stick model of CH_3OH oriented so that the C–O axis (z-axis) becomes perpendicular to the plane of the paper. The rightmost proton is the proton on the O atom side, corresponding to the position of the cross × in panel (**a**)

10.3.3.2 H_2

In [25], the Ex-MCTDHF method was applied to a one-dimensional model of an H_2 molecule. The one-dimensional model means that all particles, that is, two protons and two electrons, are restricted to move along one spatial dimension. A soft-core potential

$$V_{\mathrm{SC}}(r) = \pm\frac{e^2}{4\pi\varepsilon_0}\frac{1}{\sqrt{r^2+a^2}} \tag{10.62}$$

with soft-core parameter a is used for describing the attractive and repulsive potentials instead of the Coulomb potential. This model of H_2 contains only three degrees of freedom, that is, one for the vibrational motion, and two for the motion of the two electrons. Therefore, it is feasible to compute the total wave function of the system directly in a numerically exact way without making a product expansion as in the Ex-MCTDHF method. We may therefore compare the results of the numerically exact calculation and the results obtained by the Ex-MCTDHF method and examine the accuracy of the Ex-MCTDHF method in a rigorous way.

In the case of H_2, it is not necessary to use Slater determinants for the description of the protonic motion because there is only one vibrational degree of freedom represented by the internuclear distance R. Therefore, we can set $L_{\mathrm{p}} = 1$, $\Lambda_l = 1$, $\overline{\mathbf{R}}_{\mathrm{h}} = R$, and $C_{IJ}(\overline{\mathbf{R}}_{\mathrm{h}}, t) = C_I(R, t)$ in (10.25), so that the total wave function for H_2 is written as

$$\Psi(R, \overline{x}, t) = \sum_{I=1}^{L_e} C_I(R, t)\Phi_I(\overline{x}, t), \tag{10.63}$$

where $\overline{x}$ is the collective spatial and spin coordinate for the two electrons, and $\Phi_I(\overline{x}, t)$ is a two-electron Slater determinant. If we assume a singlet state, we should have one α and one β electron, and each Slater determinant is written as $\Phi_I(\overline{x}, t) = |\varphi_{I^\alpha}(t)\alpha\, \varphi_{I^\beta}(t)\beta|$. Therefore, once M_e electronic spatial orbitals are given, we can construct $L_e = M_e^2$ different Slater determinants.

One of the main results of [25] was that a well-converged ground state of one-dimensional H_2 can be obtained already with $M_e = 3$ spatial orbitals, corresponding to $L_e = 9$ determinants. The ground state wave function was obtained by imaginary time-propagation, and the electronic orbitals were numerically discretized using the grid method. At $M_e = 3$, the difference between the numerically exact ground state energy $\mathscr{E}_0^{(\text{exact})} = -39.34$ eV and the Ex-MCTDHF energy $\mathscr{E}_0^{(\text{Ex-MCTDHF})}$ was found to be $\mathscr{E}_0^{(\text{Ex-MCTDHF})} - \mathscr{E}_0^{(\text{exact})} \approx 10$ meV, and at $M_e = 5$, $\mathscr{E}_0^{(\text{Ex-MCTDHF})} - \mathscr{E}_0^{(\text{exact})} \approx 0.5$ meV.

Another feature of the Ex-MCTDHF wave function pointed out in [25] is that the expansion (10.63) allows us to represent the total wave function in a compact form, in the sense that the number of parameters needed to represent the wave function can be smaller than the number of parameters needed for describing a wave function using the Born-Huang expansion. If we assume for simplicity that both an electronic spatial orbital $\varphi_k(r, t)$ and a CI coefficient $C_I(R, t)$ are discretized using $\mathscr{N}$ grid points, the total number of parameters needed to specify the Ex-MCTDHF wave function becomes $\mathscr{N}_{\text{tot}} = L_e\mathscr{N} + M_e\mathscr{N} = M_e\mathscr{N}(M_e + 1)$. On the other hand, in the case of one-dimensional H_2, when we employ a Born-Huang expansion to describe the total wave function,

$$\Psi_{\text{BH}}(R, \overline{x}, t) = \sum_{I=1}^{L_e} C_I^{\text{BH}}(R, t)\Phi_I^{\text{BH}}(\overline{x}; R), \tag{10.64}$$

we would need $\mathscr{N}_{\text{tot}}^{\text{BH}} = L_e\mathscr{N} + M_e\mathscr{N}^2 = M_e\mathscr{N}(M_e + \mathscr{N})$ parameters, because each spatial orbital $\varphi_k(r; R)$ is a function of both r and R, and therefore needs $\mathscr{N}^2$ grid points for the discretization. In practical calculations, the number of grid points is typically $\mathscr{N} > 10^2$, and the number of orbitals is typically $M_e \leq 10$. Therefore, the number of parameters $\mathscr{N}_{\text{tot}}^{\text{BH}}$ required in the Born-Huang expansion (10.64) is much larger than the number of parameters $\mathscr{N}_{\text{tot}}$ required in the Ex-MCTDHF expansion (10.63). If we assume that $\mathscr{N} \gg 1$ and $M_e \ll \mathscr{N}$, then $\mathscr{N}_{\text{tot}}^{\text{BH}}/\mathscr{N}_{\text{tot}} \approx \mathscr{N} \gg 1$.

10.4 Related Methods

In this section, we give a brief account on methods similar to the Ex-MCTDHF method, describing the coupled, time-dependent motion of both electrons and nuclei

in a molecule in order that electronic and vibrational excitation are treated with a larger extent of flexibility than the BO approximation.

10.4.1 Multiconfiguration Time-Dependent Hartree Method

The multiconfiguration time-dependent Hartree (MCTDH) method [19, 20, 26] is a method originally invented for the simulation of vibrational motion of polyatomic molecules. The total vibrational wave function is written as

$$\Psi(q_1, \ldots, q_n, t) = \sum_{i_1,\ldots,i_n} C_{i_1\ldots i_n}(t)\eta_{i_1}^{(1)}(q_1, t)\ldots\eta_{i_n}^{(n)}(q_n, t), \tag{10.65}$$

where q_j represents the coordinate for the vibrational mode j, and there is a set of time-dependent basis functions $\{\eta_k^{(j)}(q_k, t)\}$ for each mode. We have assumed that there are a total of n modes. The equations of motion for the coefficients $C_{i_1\ldots i_n}(t)$ and the basis functions $\eta_k^{(j)}(q_k, t)$ can be derived using the time-dependent variational principle [20], similarly to the procedure described in Sect. 10.3.2. The MCTDH method can be used to simulate the vibrational motion of large, many-dimensional systems, as has been demonstrated in the simulation of the 15-dimensional vibrational motion of $H_5O_2^+$ [27] and the 21-dimensional vibrational motion of $C_3H_4O_2$ [28].

An extension of the MCTDH method is called the multi-layer MCTDH method [26, 29, 30]. In the multi-layer MCTDH method, the vibrational coordinates are combined into K groups of combined coordinates $\overline{\mathbf{Q}}_j$ as [26]

$$\overline{\mathbf{Q}}_1 = (q_1, \ldots, q_{k_1}),\ \overline{\mathbf{Q}}_2 = (q_{k_1+1},\ \ldots\ , q_{k_1+k_2}), \ldots, \overline{\mathbf{Q}}_K = (q_{n-k_K+1}, \ldots, q_n), \tag{10.66}$$

where k_j is the number of coordinates in group j. The wave function is written in the same way as in the original MCTDH method, but in terms of the combined coordinates $\overline{\mathbf{Q}}_j$,

$$\Psi(q_1, \ldots, q_n, t) = \sum_{i_1,\ldots,i_K} C_{i_1\ldots i_K}(t)\zeta_{i_1}^{(1)}(\overline{\mathbf{Q}}_1, t)\ldots\zeta_{i_K}^{(K)}(\overline{\mathbf{Q}}_K, t). \tag{10.67}$$

The idea of the multi-layer MCTDH method is to express each time-dependent basis function $\zeta_m^{(j)}(\overline{\mathbf{Q}}_j, t)$ as a time-dependent multiconfiguration expansion,

$$\zeta_m^{(j)}(\overline{\mathbf{Q}}_j, t) = \sum_{l_1,\ldots,l_{k_j}} C_{m,l_1\ldots l_{k_j}}^{(j)}(t)\eta_{l_1}^{(1)}(q_{a_j+1}, t)\ldots\eta_{l_{k_j}}^{(k_j)}(q_{a_j+k_j}, t), \tag{10.68}$$

where $a_j = \sum_{l=1}^{j-1} k_l$. Using the multi-layer MCTDH method, we can simulate the vibrational motion of very large systems. For example, in [31], it was shown for CH_3I embedded in calix[4]resorcinarene ($C_{28}H_{24}O_8$) that the full 189-dimensional

vibrational wave function as well as its electronic absorption spectra can be obtained by the multi-layer MCTDHF method.

In [32], it was shown that the expansion (10.65) can be applied to the coupled electro-nuclear motion of H_2^+, if q_1 represents the internuclear distance R and q_2 represents the coordinate r of the electron. If we assume a one-dimensional model like that described in Sect. 10.3.3.2, the total wave function becomes

$$\Psi(R,r,t) = \sum_{IJ} c_{IJ}(t)\chi_I(R,t)\varphi_J(r,t), \tag{10.69}$$

where $\chi_I(R,t)$ and $\varphi_J(r,t)$ are orbitals describing the nuclear and the electronic motion, respectively, and $c_{IJ}(t)$ is a time-dependent expansion coefficient. If we define an R-dependent CI coefficient by

$$C_J(R,t) = \sum_{I} c_{IJ}(t)\chi_I(R,t), \tag{10.70}$$

(10.69) can take the same form as (10.63),

$$\Psi(R,r,t) = \sum_{J} C_J(R,t)\varphi_J(r,t). \tag{10.71}$$

The difference of (10.71) and (10.63) is that the electronic wave function $\varphi_J(r,t)$ is a single-particle orbital in (10.71), while $\Phi_I(\overline{x},t)$ is a two-electron Slater determinant in (10.63).

In [32], it was concluded that an accurate time-dependent wave function of H_2^+ could be obtained when $M_e \geq 8$ electronic spatial orbitals with the same number of protonic orbitals were included in the expansion (10.69). By comparing with numerically exact wave functions obtained by a direct solution of the TDSE, it was confirmed that both the time-dependent electronic and nuclear densities as well as the high-harmonic spectra were well reproduced by the MCTDH method. This conclusion was independently confirmed in [33, 34], in which methods based on the same type of multiconfiguration expansion of the wave function shown in (10.69) were used for investigating the strong-field induced dynamics in H_2^+.

10.4.2 Multi-Configuration Electron-Nuclear Dynamics Method

The multi-configuration electron-nuclear dynamics (MCEND) method was proposed by Nest in [35] for describing time-dependent coupled electron-nuclear motion. The ansatz for the total wave function is written as

$$\Psi(\overline{\mathbf{R}}, \overline{x}, t) = \sum_{IJ} C_{IJ}(t)\xi_I(\overline{\mathbf{R}}, t)\Phi_J(\overline{x}, t), \tag{10.72}$$

where $\overline{\mathbf{R}} = (q_1, \ldots, q_n)$ is a collective coordinate for the n vibrational modes of the molecule, where q_j represents the coordinate of one vibrational mode, and $\Phi_J(\overline{x}, t)$ is a Slater determinant described as a function of the collective electronic coordinate $\overline{x}$ and t. The Slater determinant is constructed from time-dependent electronic orbitals $\varphi_k(\mathbf{r}, t)$ as in (10.20). Similarly to the MCTDH method introduced in Sect. 10.4.1, the vibrational wave functions $\xi_I(\overline{\mathbf{R}}, t)$ are written as a product of time-dependent basis functions for representing the respective vibrational modes as

$$\xi_I(\overline{\mathbf{R}}, t) = \eta^{(1)}_{I_1}(q_1, t) \ldots \eta^{(n)}_{I_n}(q_n, t). \tag{10.73}$$

The MCEND wave function ansatz (10.72) is similar to the Ex-MCTDHF ansatz (10.25) if we regard the coordinate $\overline{\mathbf{R}}_\mathrm{h}$ of the heavy nuclei as a constant. However, it should be noted that the nuclear motion is described in terms of vibrational modes in the MCEND method, whereas the motion of the protons is described by protonic orbitals in the Ex-MCTDHF method. For this reason, the Ex-MCTDHF method is considered to be suited for the simulation of molecules containing many (>3) protons as well as for the discussion of quantum effects arising from the fermionic nature of the protons, while the MCEND method could be suited for the simulation of small molecules having only a few vibrational modes. For diatomic molecules with only one vibrational degree of freedom, the nuclear motion is treated in exactly the same manner in the MCEND method and the Ex-MCTDHF method. In [36], the MCEND method was applied to investigate the time-dependent dynamics of LiH in an ultrashort laser pulse.

10.4.3 MCTDHF Method for Diatomic Molecules

Haxton et al. [37] presented a modified version of the MCTDHF method, in which the vibrational motion in a diatomic molecule is treated quantum mechanically in addition to the electronic degrees of freedom. The total wave function is written in a form similar to the Born-Huang expansion (see (10.8)) as

$$\Psi(R, \overline{x}, t) = \sum_{J} \chi_J(R, t)\Phi_J(\overline{x}, t; R), \tag{10.74}$$

where R is the internuclear distance, $\chi_J(R, t)$ is a nuclear wave function, and $\Phi_J(\overline{x}, t; R)$ is a time-dependent Slater determinant, which depends parametrically on the internuclear distance R. This parametric dependence on R makes this method different from the Ex-MCTDHF method, as can be seen from the comparison of (10.74) with (10.63). The Slater determinants are constructed from time-dependent electronic orbitals as in (10.20), but the spatial orbitals $\varphi_k(\mathbf{r}, t; R)$ depend

parametrically on R in this case. However, differently from the Born-Huang expansion, where the electronic orbitals are used to construct electronic eigenfunctions of the electronic Hamiltonian at each R (see (10.7)), in the method presented in [37], the R-dependence of the electronic spatial orbitals arises from the R-dependent basis set adopted in the expansion of the orbitals. This means that each spatial electronic orbital can be written as

$$\varphi_k(\mathbf{r}, t; R) = \sum_i c_{ki}(t) F_i(\mathbf{r}; R), \tag{10.75}$$

where $c_{ki}(t)$ is a time-dependent coefficient which is independent of R, and $F_i(\mathbf{r}; R)$ is an R-dependent basis function. The finite element method and the discrete variable representation [38] in the prolate spheroidal coordinate system were used to construct the basis functions $F_i(\mathbf{r}; R)$ in [37].

The MCTDHF method for diatomic molecules was employed in [37] to calculate accurate vibronic eigenstates of HD^+, HD, H_2, and LiH. In [39], this method was applied to the calculation of the cross section of dissociative photoionization of H_2^+. It was found that the cross section at photon energies around 30 eV, corresponding to vertical ionization, could not be well reproduced, although the cross section for large photon energies was reproduced well. To the best of our knowledge, this method has not yet been applied to coupled electro-nuclear motion in molecules in strong laser fields.

10.5 Summary

We have presented several methods that have been developed for the simulation of the coupled time-dependent motion of electrons and nuclei in molecules. In the case of the Ex-MCTDHF method, the equations of motion were derived and presented in a compact form. The two examples to which the Ex-MCTDHF method was applied have been introduced, that is, the calculations of the ground state electro-protonic wave functions of CH_3OH and H_2. In the case of CH_3OH, it was shown that the spatial proton distribution corresponding to three protons around the C atom and one proton around the O atom was reproduced well by the Ex-MCTDHF method without using a potential energy surface. Brief overviews were also given on the three related methods, the MCTDH method, the MCEND method, and the MCTDHF method for diatomic molecules.

The real advantage of the Ex-MCTDHF method is expected to appear in the real-time propagation of molecular wave functions under the influence of short and strong laser pulses. Because the Ex-MCTDHF ansatz provides a very flexible form of the total wave function, this method is suited for the simulation of extensive structural change and dissociation of a molecule in the time domain. It is expected that the Ex-MCTDHF method will be a powerful and general method for simulating ultrafast dynamics of polyatomic molecules in intense laser fields.

Acknowledgements This work was supported by JSPS KAKENHI grants no. JP15K17805, no. JP18K05024, and no. JP15H05696.

References

1. T. Okino, Y. Furukawa, P. Liu, T. Ichikawa, R. Itakura, K. Hoshina, K. Yamanouchi, H. Nakano, Coincidence momentum imaging of ultrafast hydrogen migration in methanol and its isotopomers in intense laser fields. Chem. Phys. Lett. **423**, 220 (2006)
2. T. Ando, A. Shimamoto, S. Miura, K. Nakai, H. Xu, A. Iwasaki, K. Yamanouchi, Wave packet bifurcation in ultrafast hydrogen migration in CH_3OH^+ by pump-probe coincidence momentum imaging with few-cycle laser pulses. Chem. Phys. Lett. **624**, 78 (2015)
3. M.F. Kling, C. Siedschlag, A.J. Verhoef, J.I. Khan, M. Schultze, T. Uphues, Y. Ni, M. Uiberacker, M. Drescher, F. Krausz, M.J.J. Vrakking, Control of electron localization in molecular dissociation. Science **312**, 246 (2006)
4. M. Kremer, B. Fischer, B. Feuerstein, V.L.B. de Jesus, V. Sharma, C. Hofrichter, A. Rudenko, U. Thumm, C.D. Schröter, R. Moshammer, J. Ullrich, Electron localization in molecular fragmentation of H_2 by carrier-envelope phase stabilized laser pulses. Phys. Rev. Lett. **103**, 213003 (2009)
5. V. Tagliamonti, H. Chen, G.N. Gibson, Multielectron effects in charge asymmetric molecules induced by asymmetric laser fields. Phys. Rev. Lett. **110**, 073002 (2013)
6. X. Gong, M. Kunitski, K.J. Betsch, Q. Song, L.P.H. Schmidt, T. Jahnke, N.G. Kling, O. Herrwerth, B. Bergues, A. Senftleben, J. Ullrich, R. Moshammer, G.G. Paulus, I. Ben-Itzhak, M. Lezius, M.F. Kling, H. Zeng, R.R. Jones, J. Wu, Multielectron effects in strong-field dissociative ionization of molecules. Phys. Rev. A **89**, 043429 (2014)
7. J. McKenna, A.M. Sayler, B. Gaire, N.G. Johnson, K.D. Carnes, B.D. Esry, I. Ben-Itzhak, Benchmark measurements of H_3^+ nonlinear dynamics in intense ultrashort laser pulses. Phys. Rev. Lett. **103**, 103004 (2009)
8. H. Xu, T. Okino, K. Nakai, K. Yamanouchi, S. Roither, X. Xie, D. Kartashov, M. Schöffler, A. Baltuska, M. Kitzler, Hydrogen migration and C-C bond breaking in 1,3-butadiene in intense laser fields studied by coincidence momentum imaging. Chem. Phys. Lett. **484**, 119 (2010)
9. S. Roither, X. Xie, D. Kartashov, L. Zhang, M. Schöffler, H. Xu, A. Iwasaki, T. Okino, K. Yamanouchi, A. Baltuska, M. Kitzler, High energy proton ejection from hydrocarbon molecules driven by highly efficient field ionization. Phys. Rev. Lett. **106**, 163001 (2011)
10. M. Born, R. Oppenheimer, Zur Quantentheorie der Molekeln. Ann. Phys. **389**, 457 (1927)
11. M. Born, K. Huang, *Dynamical Theory of Crystal Lattices* (Oxford University Press, Oxford, 1954)
12. B. Jiang, J. Li, H. Guo, Potential energy surfaces from high fidelity fitting of ab initio points: the permutation invariant polynomial—neural network approach. Int. Rev. Phys. Chem. **35**, 479 (2016)
13. F. Martín, J. Fernández, T. Havermeier, L. Foucar, T. Weber, K. Kreidi, M. Schöffler, L. Schmidt, T. Jahnke, O. Jagutzki, A. Czasch, E.P. Benis, T. Osipov, A.L. Landers, A. Belkacem, M.H. Prior, H. Schmidt-Böcking, C.L. Cocke, R. Dörner, Single photon-induced symmetry breaking of H_2 dissociation. Science **315**, 629 (2007)
14. G. Sansone, F. Kelkensberg, J.F. Pérez-Torres, F. Morales, M.F. Kling, W. Siu, O. Ghafur, P. Johnsson, M. Swoboda, E. Benedetti, F. Ferrari, F. Lépine, J.L. Sanz-Vicario, S. Zherebtsov, I. Znakovskaya, A. L'Huillier, M.Y. Ivanov, M. Nisoli, F. Martín, M.J.J. Vrakking, Electron localization following attosecond molecular photoionization. Nature (London) **465**, 763 (2010)
15. T. Kato, K. Yamanouchi, Time-dependent multiconfiguration theory for describing molecular dynamics in diatomic-like molecules. J. Chem. Phys. **131**, 164118 (2009)
16. J. Zanghellini, M. Kitzler, C. Fabian, T. Brabec, A. Scrinzi, An MCTDHF Approach to multielectron dynamics in laser fields. Laser Phys. **13**, 1064 (2003)

17. T. Kato, H. Kono, Time-dependent multiconfiguration theory for electronic dynamics of molecules in an intense laser field. Chem. Phys. Lett. **392**, 533 (2004)
18. E. Lötstedt, T. Kato, K. Yamanouchi, in *Ultrafast Intense Laser Science XIII, Vol. 116 of Springer Series in Chemical Physics*, ed. by K. Yamanouchi, W.T. Hill III, G.G. Paulus (Springer International Publishing, Switzerland, 2017), pp. 15–40 (in progress)
19. H.-D. Meyer, U. Manthe, L. Cederbaum, The multi-configurational time-dependent Hartree approach. Chem. Phys. Lett. **165**, 73 (1990)
20. M. Beck, A. Jäckle, G. Worth, H.-D. Meyer, The multiconfiguration time-dependent Hartree (MCTDH) method: a highly efficient algorithm for propagating wavepackets. Phys. Rep. **324**, 1 (2000)
21. T. Helgaker, P. Jørgensen, J. Olsen, *Molecular Electronic-Structure Theory* (Wiley, Hoboken, NJ, 2000)
22. P.A.M. Dirac, Note on exchange phenomena in the Thomas atom. Math. Proc. Camb. Phil. Soc. **26**, 376 (1930)
23. P.-O. Löwdin, P.K. Mukherjee, Some comments on the time-dependent variation principle. Chem. Phys. Lett. **14**, 1 (1972)
24. T. Kato, K. Yamanouchi, Protonic structure of CH_3OH described by electroprotonic wave functions. Phys. Rev. A **85**, 034504 (2012)
25. Y. Ide, T. Kato, K. Yamanouchi, Non-Born-Oppenheimer molecular wave functions of H_2 by extended multi-configuration time-dependent Hartree-Fock method. Chem. Phys. Lett. **595–596**, 180 (2014)
26. U. Manthe, Wavepacket dynamics and the multi-configurational time-dependent Hartree approach. J. Phys. Cond. Matter **29**, 253001 (2017)
27. V. Oriol, G. Fabien, M. Hans-Dieter, Dynamics and infrared spectroscopy of the protonated water dimer. Angew. Chem. Int. Ed. **46**, 6918 (2007)
28. M.D. Coutinho-Neto, A. Viel, U. Manthe, The ground state tunneling splitting of malonaldehyde: accurate full dimensional quantum dynamics calculations. J. Chem. Phys. **121**, 9207 (2004)
29. H. Wang, M. Thoss, Multilayer formulation of the multiconfiguration time-dependent Hartree theory. J. Chem. Phys. **119**, 1289 (2003)
30. U. Manthe, A multilayer multiconfigurational time-dependent Hartree approach for quantum dynamics on general potential energy surfaces. J. Chem. Phys. **128**, 164116 (2008)
31. T. Westermann, R. Brodbeck, A.B. Rozhenko, W. Schoeller, U. Manthe, Photodissociation of methyl iodide embedded in a host-guest complex: a full dimensional (189D) quantum dynamics study of CH_3I@resorc[4]arene. J. Chem. Phys. **135**, 184102 (2011)
32. C. Jhala, M. Lein, Multiconfiguration time-dependent Hartree approach for electron-nuclear correlation in strong laser fields. Phys. Rev. A **81**, 063421 (2010)
33. A. Hanusch, J. Rapp, M. Brics, D. Bauer, Time-dependent renormalized-natural-orbital theory applied to laser-driven H_2^+. Phys. Rev. A **93**, 043414 (2016)
34. R. Anzaki, T. Sato, K.L. Ishikawa, A fully general time-dependent multiconfiguration self-consistent-field method for the electron-nuclear dynamics. Phys. Chem. Chem. Phys. **19**, 22008 (2017)
35. M. Nest, The multi-configuration electron-nuclear dynamics method. Chem. Phys. Lett. **472**, 171 (2009)
36. I.S. Ulusoy, M. Nest, The multi-configuration electron-nuclear dynamics method applied to LiH. J. Chem. Phys. **136**, (2012)
37. D.J. Haxton, K.V. Lawler, C.W. McCurdy, Multiconfiguration time-dependent Hartree-Fock treatment of electronic and nuclear dynamics in diatomic molecules. Phys. Rev. A **83**, 063416 (2011)
38. L. Tao, C.W. McCurdy, T.N. Rescigno, Grid-based methods for diatomic quantum scattering problems: a finite-element discrete-variable representation in prolate spheroidal coordinates. Phys. Rev. A **79**, 012719 (2009)
39. D.J. Haxton, K.V. Lawler, C.W. McCurdy, Qualitative failure of a multiconfiguration method in prolate spheroidal coordinates in calculating dissociative photoionization of H_2^+. Phys. Rev. A **91**, 062502 (2015)